Femtochemistry of the liquid phase laser-induced harpoon reaction between Cl_2 and Xe. Observation of bond formation in real time

R. Zadoyan and V.A. Apkarian
Department of Chemistry, University of California, Irvine, CA 92717, USA

Received 11 February 1993; in final form 18 March 1993

The liquid phase, two-photon induced intermolecular charge transfer transition, $Cl_2 + Xe + 2h\nu \rightarrow Xe^+Cl_2^-$, in which the photon is resonant with the dissociative $Cl_2(^1\Pi_u)$ intermediate state, is shown to proceed on a time scale shorter than 100 fs. The process is therefore classified as a coherent, cooperative absorption. The subsequent evolution of the harpoon reaction, $Xe^+Cl_2^- \rightarrow Xe^+Cl^- + Cl$, which in liquid Xe further proceeds to form $Xe_2^+Cl^-$, is followed in time by stimulating the radiative dissociation of Xe^+Cl^-. While the formation of Xe^+Cl^- cannot be temporally resolved, the triatomic bond forms in 330 fs.

1. Introduction

With the advent of femtosecond laser technologies, real-time observation of the evolution of chemical reactions, the breaking and making of chemical bonds, has become a reality (for a review, see ref. [1]). Bimolecular reactions represent a particularly attractive target of such investigations, since they allow the study of a complete reaction, allowing the observation of bond formation between reagents [2]. This challenge has been met by elegant gas phase studies most successfully by isolating reagents as van der Waals hetero-complexes, such as CO_2:HI, in molecular beams [3,4]. Given the relevance to chemistry, and the conceptual difficulties associated with many-body interactions, probing of elementary reaction steps in condensed phases is rather instructive. The laser-induced harpoon reaction between solvent and solute molecules enables such studies. The approach consists of following reaction dynamics subsequent to sudden promotion of reagents from covalent to ionic potential energy surfaces. In the present work, electron transfer between solvent Xe and molecular Cl_2 is affected by a coherent two-photon absorption, a process which we discuss in some depth. The reaction evolves on the ionic hypersurfaces to first form the diatomic exciplex, Xe^+Cl^-, and subsequently, by reacting with a second solvent atom, to form the stable charge transfer complex, $Xe_2^+Cl^-$. Given the heavy masses of the reagents, and the soft intermolecular potential between Xe^+Cl^- and solvent Xe, the formation of the triatomic bond can be followed in real time, with the time resolution of $\approx 10^{-13}$ s available in these experiments.

The two-photon laser-induced harpoon reaction between molecular halogens and rare gas atoms has been studied extensively. The experimental gas phase studies were recently reviewed by Nelson, Setser and Qin [5], an overview of the early experimental studies in condensed phases exists [6] and theoretical treatments of different aspects of the process have been given under different headings: cooperative transitions [7,8], laser-assisted collisional processes [9], radiative collisions [10] are examples. Many variants of the process can be classified and demonstrated. For example, two distinct types of sequential photo-excitations have been demonstrated in gas, liquid, and fluid phases [11–13]:

(a) Photodissociation followed by photo-association, viz.

$$MX + h\nu \rightarrow M + X, \quad (1a)$$

$$X + Rg + h\nu \rightarrow Rg^+X^-, \quad (1b)$$

in which the second photon is absorbed by either a transient collision complex or by a van der Waals complex trapped in its potential minimum.

(b) Excitation of a bound molecular intermediate state, followed by intermolecular charge transfer excitation, viz.

$$X_2 + h\nu \rightarrow X_2^*, \qquad (2a)$$

$$X_2^* + Rg + h\nu \rightarrow [Rg^+X_2^-] \rightarrow Rg^+X^- + X, \qquad (2b)$$

the energetics of which has been discussed in some detail for the case of Br_2 in liquid Xe [6,12]. This process has been recently utilized in gas phase I_2/Xe as an example of bimolecular femtochemistry [14].

While the sequential two-photon processes have been demonstrated by time-delay measurements, coherent two-photon contributions have been implicated by indirect arguments. Of particular interest in this category are transitions in which the intermediate state resonance is dissociative. In the example considered here, the two-photon-induced harpoon reaction between Cl_2 and Xe, the photon is chosen to be resonant with the dissociative $^1\Pi_u \leftarrow X(^1\Sigma_g)$ absorption of Cl_2. Accordingly, the process may be described as either

$$Xe + Cl_2 + 2h\nu \rightarrow Xe^+Cl_2^- \rightarrow Xe^+Cl^- + Cl$$

$$\xrightarrow{Xe} Xe_2^+Cl^- + Cl \qquad (3)$$

or

$$Xe + Cl_2 [\xrightarrow{h\nu} XeCl + Cl \xrightarrow{h\nu}] Xe^+Cl^- + Cl$$

$$\xrightarrow{Xe} Xe_2^+Cl^- + Cl, \qquad (4)$$

the distinction being in the entrance channel of the reaction. The process of eq. (3) is a coherent two-photon absorption leasing to charge transfer between Xe and molecular Cl_2. The molecular ion then undergoes rapid dissociation into Cl^- and Cl, and the exciplex formation occurs by Coulombic attraction between nascent ions. The process of eq. (4) is in effect sequential. The first photon leads to the dissociative surface of Cl_2. The system evolves on this surface leading to a collision between Cl and Xe atoms at which time the second photon induces a charge transfer between the colliding pair of atoms. A pictorial illustration of the two processes is given in figs. 1 and 2. Since in the mechanism of eq. (3) the photon is resonant with a dissociative intermediate state, fast time evolution of nuclear coordinates on this surface is to be expected. In that sense, the distinction between the two mechanisms is one of time scales, one that can in principle be resolved by experiments using short pulse lasers.

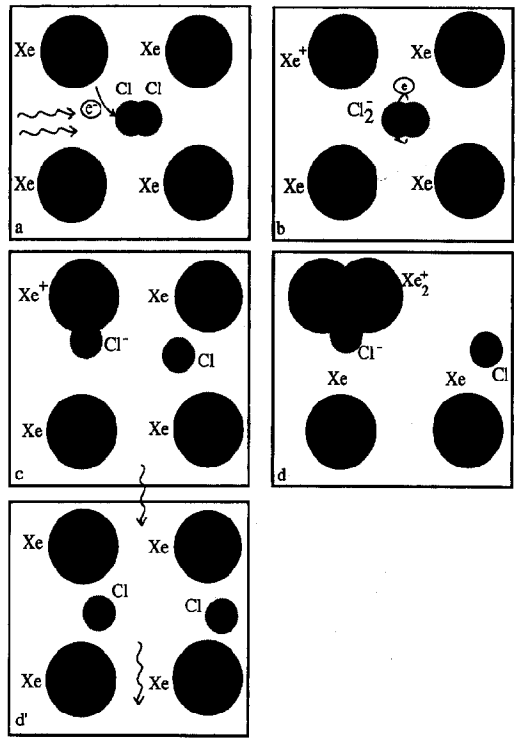

Fig. 1. Coherent two-photon-induced harpoon reaction. Two photons are absorbed to transfer an electron from Xe to Cl_2 without significant evolution of nuclear coordinates (a). The electron transfer is to the molecular Cl_2 anti bonding π orbital (b). The harpooning occurs with concomitant dissociation of Cl_2^- and formation of Xe^+Cl^- bonds (c). The triatomic exciplex is formed by compression of the separation between Xe^+Cl^- and solvent Xe atom (d). This process can be interrupted by stimulating the radiative dissociation of Xe^+Cl^- ((c)→(d')).

In liquid Xe the final outcome of the harpoon reaction is the formation of the triatomic exciplex, $Xe_2^+Cl^-$. The reaction is assumed to proceed by initial formation of the diatomic, Xe^+Cl^- exciplex, and subsequent formation of the triatomic, as indicated in the illustrations of figs. 1 and 2. The diatomic exciplex, which is the species responsible for the common gas phase 308 nm laser, has a large transition dipole connecting it to the covalent, repulsive XeCl(X) ground state. This transient species should therefore be possible to monitor in real time by stim-

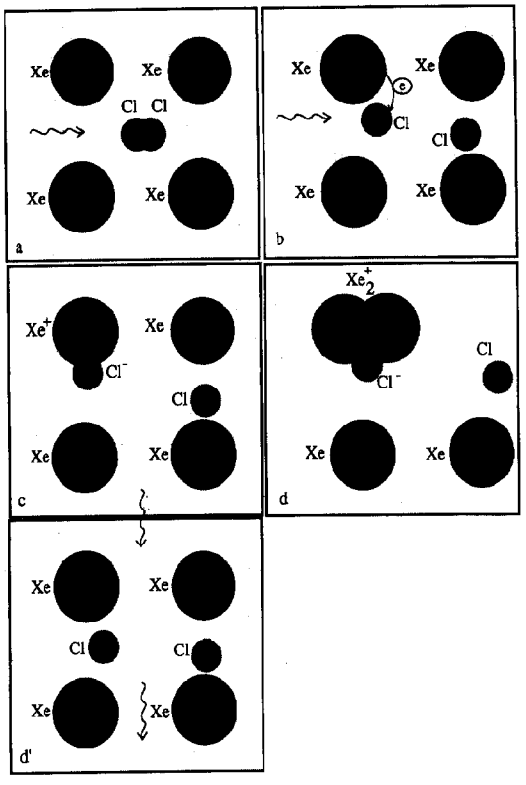

Fig. 2. Sequential two-photon-induced harpoon reaction. The first photon is absorbed by Cl_2 (a). Upon dissociation, a second photon is absorbed by the Cl–Xe collision complex (b) to form the diatomic exciplex (c). The latter may either further react to form the triatomic exciplex (d) or may be induced to undergo radiative dissociation (d').

ulating its radiative dissociation. This is the process that leads from panels (c) to (d') in the pictorial illustrations.

The above establishes the experimental paradigm used in the present work to follow bond formation, in real time, in the liquid phase. The entire process is followed at a single wavelength, at 320 nm, with a laser of typical pulse widths of 100–150 fs. At low fluences, the two-photon absorption time scale is established by monitoring the $Xe_2^+Cl^-$ emission. At high fluence, the reaction is arrested by stimulating the radiative dissociation of the diatomic exciplex. Since this intermediate is destroyed by formation of the triatomic, its lifetime yields the time scale for bond formation between the diatomic solute, Xe^+Cl^-, and a solvent Xe atom.

2. Experimental

The experiments are conducted in a 4 cm long T cell, constructed of rhodium plated Be:Cu. Sapphire windows of 3 mm thickness are used on all sides. The cell is mounted on the tip of a cryostat, fitted with a resistive heater and thermocouple, enabling temperature control between 30 and 300 K. An all monel manifold is used for the introduction of gases to the cell. An inconel capacitance manometer is used to measure pressure. The experiments were carried out in Cl_2/Xe solutions varying between 1:5000 to 1:30000.

The laser system used for these measurements is assembled from mostly commercial parts. The doubled output of a 76 MHz mode-locked YAG laser (Coherent, Antares) is used to pump a dye laser with active feedback (Coherent Satori). Kiton red is used as the dye, and malachite green is used as the saturable absorber. At 640 nm, pulses as short as 80 fs have been obtained from this system. A 30 Hz regenerative amplifier (Continuum) is used to amplify the dye output in a three stage dye amplifier. The amplified dye is then doubled in a BBO crystal. The negative dispersion of the output of the dye laser is adjusted to be compensated by the dye amplifier and all optical elements leading to the center of the experimental cell. The 320 nm beam, ≈ 1 μJ/pulse, is split and recombined after a delay line. They are colinearly focused in the cell with a single lens. Two retroreflectors are mounted on the moving stage of the delay line, one for the 320 nm beam and one for the 640 nm dye fundamental. The arrangement enables the simultaneous recording of fluorescence from the cell and the auto correlation of the amplified dye laser. The pulse width of the 320 nm beam is not measured directly.

The experiment consists of following the $Xe_2^+Cl^-$ emission at 570 nm from the focal volume. The measurements are carried out as a function of delay between the split beams, at different laser fluences.

3. Results and discussion

3.1. The two-photon absorption

Under mild focusing conditions, and in dilute solutions – 1 $\mu J/cm^2$, Cl_2:Xe=1:30000 – the $Xe_2^+ Cl^-$ emission shows a peak centered at zero delay. This normal signal is illustrated in the top panel of fig. 3. A fwhm as narrow as 160 fs is observed for this signal, which is quite close to the auto correlation of the narrowest pulses obtained from our system. The width of the peak is typically 10% broader than the pulse width of the 640 nm laser. The latter is measured by collinear auto correlation. We suspect that, due to uncontrollable dispersion effects in the doubling process and the optical train leading to the center of the cell, the 320 nm pulses are at least 10% broader than the 640 nm pulses. The power dependence of the fluorescence peak varies between 2 and 1.6 as a function of increasing intensity when a lens of 50 cm focal length is used. Since in effect we observe two-photon-induced signals that closely follow the auto correlation of the laser, the two photons must be absorbed on a time scale significantly shorter than the laser pulse width, a time scale shorter than ≈ 100 fs.

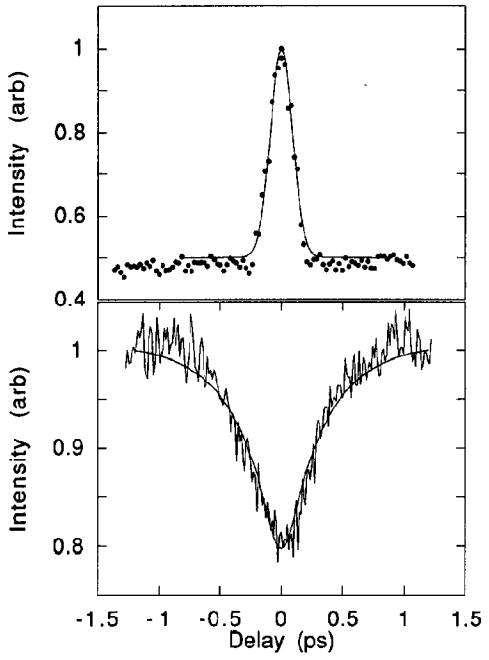

Fig. 3. $Xe_2^+ Cl^-$ emission as a function of delay between 320 nm pulses. At low intensities, 20 $\mu J\ cm^{-2}$, a laser limited positive peak is observed at zero delay (top panel). At high intensities, 2 $mJ\ cm^{-2}$, the signal inverts and shows a finite response time (lower panel). The signals are simulated by numerical integration, using the kinetic scheme of eq. (5) and by convolution of 150 fs pulses.

Evidently, the two-photon-induced charge transfer between Xe and chlorine proceeds prior to significant stretching of the Cl–Cl bond on the $^1\Pi$ dissociative surface, i.e. a mechanism consistent with the coherent, cooperative absorption implied by eq. (3).

It is possible to establish that the observed signal is inconsistent with the mechanism of eq. (4), i.e. Cl_2 dissociation followed by photo-association of the Cl–Xe collision pair. The vertical nature of photo-association requires Franck–Condon overlap between the free XeCl and bound Xe^+Cl^-. This imposes the requirement of absorption from the vicinity of turning points: either at the Cl–Cl repulsive wall, or at the Xe–Cl repulsive wall. The first would imply very small propagation of the free state in time, i.e. better described by eq. (3) (fig. 1). For the second process, an estimate of the time for first collision (TFFC) for Cl atoms born on the repulsive $^1\Pi$ surface should be considered. TFFC is a distribution function in time, determined mainly by the Cl–Xe pair distribution and collision impact parameters. Noting the similarity between Xe–Xe and Xe–Cl_2 van der Waals potentials [15], to a good approximation, we may assume that the Xe–Xe 6–12 potential determines the structure of the liquid. The first peak in the radial distribution function of such a liquid occurs at $\approx 1.1\sigma$ with fwhm at $\pm 0.1\sigma$ [16]; which translates to a Xe–Cl_2 nearest-neighbor distribution of 4.7 ± 0.44 Å. At these temperatures, a flat angular distribution between the Cl_2 molecular axis and nearest-neighbor Xe atoms is to be expected. At an average coordination number of 10, this implies a solid angle spanning 1.25 sr – a half angle of the cone of $\approx 35°$. Taking both angular and radial distributions into account in sampling initial conditions, the TFFC is computed by numerical integration of the classical equations of motion. An exponentially repulsive $Cl_2(^1\Pi)$ potential, which reproduces the absorption spectrum of Cl_2 in liquid Xe [17], is used: $V = 312 \exp(-2.77r)$, in eV Å units. For the covalent Xe–Cl potential, the Morse form with parameters

derived from molecular beam studies [18], is used: $V=0.0346\exp[\beta(1-r/r_m)]$, $\beta=5.2$ Å^{-1}, $r_m=3.23$ Å.

At 320 nm, Cl_2 is born on the repulsive excited surface, 1.38 eV above the dissociation limit, at an internuclear separation of 1.956 Å. With this initial kinetic energy, Cl atoms collide with Xe at an internuclear separation of ≈ 2 Å. Collisions with the first shell Xe atoms yield a TFFC skewed to longer times, with a peak centered at 125 fs, and half height at 90 fs. Nearly 50% of the Cl atoms escape the first solvation shell to collide with second-shell atoms at a distance of 2σ, and a delay time of 280 fs. Convolution of the first shell TFFC with the laser pulse of 150 fs, yields a response function of fwhm 300 fs, significantly broader than the response function observed in fig. 3a. Using the complete TFFC distribution, including second-shell collisions, would of course predict an even broader response function. We conclude, that with the classical interpretation of a collision, the observed signal is inconsistent with the mechanism of eq. (4) (fig. 2).

3.2. Observation of bond formation

At high intensities, at ≈ 2 mJ/cm^2, the fluorescence peak at zero delay inverts. An example is shown in the lower panel of fig. 3. The inverted signal is significantly broader than the normal, and therefore implies interaction of radiation with an intermediate state of finite lifetime. A rather obvious mechanism for inversion of the signal at high powers is the radiation-induced depletion of the intermediate state leading to the observable product, $Xe_2^+Cl^-$. Two-photon access of an intermediate state, and its depletion by a one-photon excitation in competition with the channel leading to the product, is the minimal model that explains the observed power dependence of the signal. The kinetics can be reduced to

$$A \xrightarrow{\alpha} B, \quad \alpha=\sigma^{(2)}I^2, \tag{5a}$$

$$B \xrightarrow{\beta} C, \quad \beta=\sigma^{(1)}I, \tag{5b}$$

$$B \xrightarrow{k} P, \tag{5c}$$

in which C is a dark state; P is the fluorescent state; I is the experimentally determined photon flux; and $\sigma^{(2)}$ and $\sigma^{(1)}$ are two- and one-photon absorption cross sections, respectively. The data can be fit by numerical integration of the rate expressions implied by eq. (5), and convolution of the laser pulses. The fits in fig. 3 for both the normal and inverted signals were made using Gaussian pulses of 150 fs duration, $\sigma^{(2)}=10^{-43}$ cm^4 s, $\sigma^{(1)}=10^{-16}$ cm^2, and $k=330$ fs, and the experimentally measured intensities of 15 μJ cm^{-2} for the normal signal and 1.8 mJ cm^{-2} for the inverted signal. The model parameters are well determined. The fit to the normal signal fixes the pulse width of the laser, and $\sigma^{(2)}$. The fit to the inverted signal, depth and width of the modulation, fix $\sigma^{(1)}$ and k. The inversion is in effect due to saturation of Cl_2 molecules in the focal volume, such that the rate of the one-photon-induced process, $\beta B(t)$, becomes larger than the two-photon-driven process, $\alpha A(t)$.

The derived two-photon cross section is in acceptable agreement with prior determinations: 7.4×10^{-45} cm^4 s^{-1} in the gas phase [5], 1.6×10^{-44} cm^4 s^{-1} in the liquid phase [6], and 1×10^{-43} cm^4 s^{-1} in solid Xe [19]. Enhancement for this transition in condensed media, as a function of density, is to be expected. This has been previously discussed both in the context of quantum electrodynamics descriptions of cooperative processes [7], and in analogy [20] with the "giant two-photon absorption" [21] mechanisms of excitonic molecules in solids.

There is little ambiguity in the identification of B in the kinetic scheme of eq. (5) as Xe^+Cl^-, and reaction (5b) as the stimulated radiative dissociation of the diatomic exciplex,

$$Xe^+Cl^- \xrightarrow{h\nu=320\text{ nm}} Xe+Cl. \tag{6}$$

At 320 nm, this optical transition is the only one with sufficient oscillator strength to yield the observed cross section. The equilibrated XeCl(B→X) emission in liquid Ar peaks at 350 nm, with a fwhm of 17 nm [2]. The solvation corrected radiative lifetime for this state can be estimated as 5 ns [19]. Accordingly, a stimulated emission cross section of 2.5×10^{-16} cm^2 can be deduced, in good agreement with the extracted value for $\sigma^{(1)}$.

According to the kinetic scheme, Xe^+Cl^- disappears in 330 fs. Noting that the wavelength of the down stimulating pulse remains in the window of emission from fully relaxed Xe^+Cl^- in the liquid

phase [6], it becomes clear that the signal decay is not due to vibrational relaxation within the diatomic exciplex, or due to fast evolution of Franck–Condon factors tying it to the repulsive ground state. Disappearance by reaction, by formation of the bond between Xe^+Cl^- and Xe to yield the triatomic exciplex, is the remaining decay channel. This involves the compression of the Xe–Xe separation from its liquid phase nearest-neighbor value to that of the Xe–Xe bond length in $Xe_2^+Cl^-$, of 3.2 Å [22,23]. The time scale of this process can be estimated by noting that the bond compression occurs on the attractive potential due to dipole–induced dipole forces – between the nascent Xe^+Cl^- dipole and the polarizable Xe. Accordingly, the bond formation time scale can be estimated from the classical, one-dimensional equation of motion, on an R^{-6} attractive potential as

$$dR = at\,dt = -\frac{1}{M}\frac{dV}{dR}t\,dt = -\frac{3\alpha\mu^2}{MR^7}t\,dt\,, \qquad (7a)$$

in which the motion is assumed to start from rest. Integration of (7a) yields

$$R_f^8 - R_i^8 = -\frac{12\alpha\mu^2}{M}t^2\,, \qquad (7b)$$

in which $\mu = 12$ D is the dipole of Xe^+Cl^- [24], $\alpha = 4$ Å^3 is the polarizability of Xe, $M = 73.3$ amu is the reduced mass of the system. It can therefore be calculated that a bond compression from $R_i = 4.7$ Å to $R_f = 3.2$ Å will occur in 315 fs. The observed time scale of 330 fs is in good agreement with this estimate.

For the sake of clarity, we summarize the above developed picture by referring to portions of the relevant potential energy surfaces which are schematized in fig. 4. The surfaces are created using the known pair potentials, and assuming pairwise additivity. The two-photon-induced charge transfer involves three surfaces: $Xe–Cl_2(X)$, $Xe–Cl_2(^1\Pi)$, $Xe^+–Cl_2^-$. The process creates Cl_2^- on its repulsive wall, ≈ 1.5 eV above its dissociation limit. The total time evolution required to reach the Xe^+Cl^- configuration (a compression of ≈ 0.4 Å along this coordinate) from which the radiative dissociation can be stimulated is not resolvable in our experiments – it is less than 100 fs. Although dominated by Cl^-, in principle motion on both the intermediate and final states of the optical transition contributes to this evolution. Passage from the Xe^+Cl^- configuration, which can be stimulated to undergo radiative dissociation, to the minimum of the ionic surface at the triatomic configuration, is due to heavy fragments traveling a distance of ≈ 1.4 Å, on a soft R^{-6} potential, and starting from rest.

4. Conclusions

The possible contribution of coherent versus sequential absorption to two-photon-induced harpoon reactions has been considered in the past in gas phase static cell experiments [5,25], in $Xe:Cl_2$ clusters formed in molecular beams [26], in high pressure and super critical Xe [13], in liquid Xe [27], in solid Xe [19] including studies under high pressure [28]. Although in all these studies the notion of a coherent process is used to explain results, and despite the fact that there is agreement between two-photon cross sections measured in the gas and condensed phases, direct demonstration of coherence has not yet been given [5]. In this Letter, we report the direct observation that the two-photon charge transfer absorption can be induced on a time scale less than 100 fs. It is furthermore established that the observed process is not consistent with sequential photodissociation followed by photo-association. Such a process would require capture of Cl–Xe collision pairs. The time for first collision, first and second shell collisions, would stretch the system response to several hundred femtoseconds. In short, we establish the validity of the classification of this two-photon, two-electron transition as a cooperative absorption [7].

The two-photon-induced intermolecular charge transfer transition serves as a sudden entrance channel to the harpoon reaction between Xe and Cl_2 in condensed phases. The rearrangement of charge from $Xe^+(Cl_2)^-$, in which the electron is in the molecular antibonding σ^* orbital, to Xe^+Cl^-Cl, in which the electron is localized on one of the Cl atoms, proceeds on a time scale too short to be directly observed with our apparatus. Within our experimental time resolution, Xe^+Cl^- is born instantaneously. It is not clear whether this charge rearrangement is controlled by the nuclear dynamics, i.e. the dissociation of Cl_2^-, or strictly by the pairing of charges.

In liquid Xe, the diatomic exciplex is transient, it

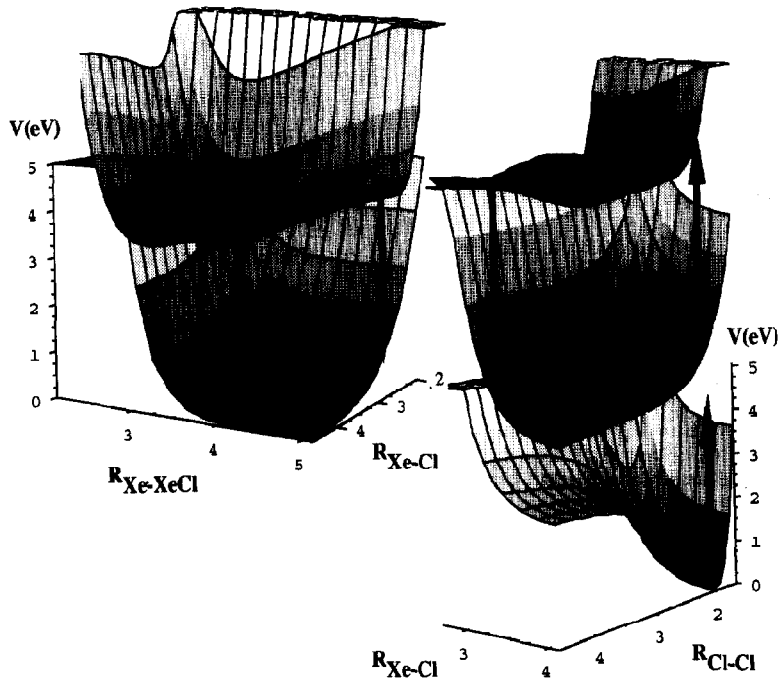

Fig. 4. Potential energy surfaces for the two-photon-induced harpoon reaction between Xe and Cl_2. The excitation is illustrated with the up-arrows, over the three stacked surfaces. The two-photon excitation promotes the system from the covalent Xe–Cl_2 ground state to the ionic $Xe^+Cl_2^-$ surface, with the purely repulsive Xe–$Cl_2(^1\Pi)$ surface acting as an intermediate resonance. In the collinear geometry assumed in the figure, the system is born at $R(Cl_2^-) = 1.95$ Å and $R(ClXe) = 3.6$ Å, which corresponds to an energy of ≈ 1.5 eV above the dissociation limit of the molecular ion. The system evolves by separation of the Cl–Cl^- coordinate, and by contraction of the Xe^+Cl^- coordinate. The radiative dissociation of the nascent Xe^+Cl^- can be stimulated (down-arrows). If not interrupted, the system would evolve on this relatively flat surface to form the triatomic exciplex, $Xe_2^+Cl^-$. The latter relaxes radiatively (shown by wavy arrow). The two down-arrows are meant to represent the same configuration. The surfaces are vertically separated from each other for the sake of visibility. All distances are in Å, and energies are in eV.

will react with another Xe atom to form the triatomic $Xe_2^+Cl^-$. This reaction is observed to proceed on a time scale of 330 fs. The time scale can be rationalized as that of the compression of the Xe–Xe bond under the influence of dipole–induced dipole forces.

The experimental data were interpreted based on simple classical kinematics. Although it is felt that the treatment captures the essence of the dynamics, as a uniquely useful method of following elementary steps in chemistry in condensed phases in real time, photo-induced harpoon reactions deserve a more thorough and rigorous treatment by both theory and experiment.

Acknowledgement

This research was supported by a grant from the National Science Foundation, ECS-8914321, and by the US Air Force Phillips Laboratory under contract S04611-90-K-0035. We appreciate the assistance given by D.G. Imre and M. Hill during these experiments. We thank AHZ for his suggested improvements to this manuscript.

References

[1] A.H. Zewail, Science 242 (1988) 1645;
L.R. Khundkar and A.H. Zewail, Ann. Rev. Phys. Chem. 41 (1990) 15.

[2] I.R. Sims, M. Gruebele, E.D. Potter and A.H. Zewail, J. Chem. Phys. 97 (1992) 4127.
[3] N.F. Scherer, L.R. Khundkar, R.B. Bernstein and A.H. Zewail, J. Chem. Phys. 87 (1987) 1451;
N.F. Scherer, C. Sipes, R.B. Bernstein and A.H. Zewail, J. Chem. Phys. 92 (1990) 5239.
[4] S.I. Ionov, G.A. Bucker, C. Jacques, L. Valachovic and C. Wittig, J. Chem. Phys. 97 (1992) 9486.
[5] T.O. Nelson, D.W. Setser and J. Qin, J. Phys. Chem, to be published.
[6] M.E. Fajardo, R. Withnall, J. Feld, F. Okada, W. Lawrence, L. Wiedeman and V.A. Apkarian, Laser Chem. 9 (1988) 1.
[7] D.L. Andrews and K.P. Hopkins, Advan. Chem. Phys. 77 (1990) 39.
[8] D.L. Dexter, Phys. Rev. 126 (1962) 1962.
[9] T.F. George and K.-S. Lam, Chem. Rev. 87 (1987) 155;
H.-W. Lee and T.F. George, Phys. Rev. A 35 (1987) 4977;
H.F. Arnoldus, T.F. George, K.-S. Lam, J.F. Scipione, P.L. Dervries and J.-M. Yuan, in: Laser applications in physical chemistry, ed. D.K. Evans (Marcel Dekker, New York, 1989) p. 329.
[10] S.I. Yakovlenko, Soviet J. Quantum Electron. 8 (1978) 151.
[11] A.W. McCown and J.G. Eden, J. Chem. Phys. 81 (1984) 2933.
[12] W.G. Lawrence and V.A. Apkarian, Israel J. Chem. 30 (1990) 135.
[13] F. Okada and V.A. Apkarian, J. Chem. Phys. 94 (1991) 133.
[14] E.D. Potter, J.L. Herek, S. Pedersen, Q. Liu and A.H. Zewail, Nature 355 (1992) 66.
[15] C.R. Bieler, K.E. Spence and K.C. Janda, J. Phys. Chem. 95 (1991) 5058;
C.R. Bieler and K.C. Janda, J. Am. Chem. Soc. 112 (1990) 2033.
[16] L. Verlet, Phys. Rev. 165 (1968) 201.
[17] M.E. Fajardo, V.A. Apkarian, A. Moustakas, H. Kreuger and E. Weitz, J. Phys. Chem. 92 (1988) 357.
[18] C.H. Becker, J.J. Valentini, P. Casavecchia, S.J. Sibener and Y.T. Lee, Chem. Phys. Letters 61 (1979) 1.
[19] M.E. Fajardo and V.A. Apkarian, J. Chem. Phys. 85 (1986) 5660.
[20] H. Kunttu, J. Feld, R. Alimi, A. Becker and V.A. Apkarian, J. Chem. Phys. 92 (1990) 4856.
[21] M. Ueta, H. Kanzaki, K. Kobayashi, Y. Toyozawa and E. Hanamura, in: Springer series in solid state sciences, Vol. 60. Excitonic processes in solids (Springer, Berlin, 1986) ch. 2, 3.
[22] D.L. Huestis, G. Marowsky and F.K. Tittel, in: Topics in applied physics, Vol. 30. Excimer lasers, ed. Ch.R. Rhodes (Springer, Berlin, 1984).
[23] H.H. Michels, R.H. Hobbs and L.A. Wright, J. Chem. Phys. 69 (1978) 5151.
[24] P.J. Hay and T.H. Dunning, J. Chem. Phys. 69 (1978) 2209.
[25] J.K. Ku, G. Inoue and D.W. Setser, J. Phys. Chem. 87 (1983) 2989.
[26] M. Boivineau, J. Le Calve, M.C. Castex and C. Jouvet, Chem. Phys. Letters 128 (1986) 528; J. Chem. Phys. 84 (1986) 4712;
C. Jouvet, M. Boivineau, M.C. Duval and B. Soep, J. Phys. Chem. 91 (1987) 5416.
[27] L. Wiedeman, M.E. Fajardo and V.A. Apkarian, J. Phys. Chem. 92 (1988) 342;
F. Okada, L. Wiedeman and V.A. Apkarian, J. Phys. Chem. 93 (1989) 1267.
[28] A.I. Katz and V.A. Apkarian, J. Phys. Chem. 94 (1990) 6671.